Photon Upconversion Nanoparticles: PLIM and FRET Application

Yuansheng Sun, Ulas Coskun and Shih-Chu Liao
ISS

1 Introduction to the Photon Upconversion Nanoparticles

Photon upconversion is a process of sequential absorption of multi-photons (two or more photons) with the emission occurring at a shorter wavelength than the excitation wavelength [1]. A typical photon upconversion features anti-Stokes type emission, which usually converts infrared light to visible light [2] [3] [4] [5] [6] by adding d-block or f-block elements, such as Lanthanide –doped materials[1], Ti^{2+}, Re^{4+} -doped materials [4], CdSe semiconductor nanocrystals [5] or lead sulphide colloidal nanocrystals [6]) into materials.

There are different mechanisms, such as Energy Transfer Upconversion (ETU), Excited-State Absorption (ESA) or Photon Avalanche (PA), to facilitate photon upconversion. The doped material can be as big as a fiber or as small as nano-particles. Another benefit of photon upconversion is relatively low intensity required for the excitation. This introduces a wide range of applications, such as medical imaging [2] or differential Cancer Bioimaging in vivo [7].

The Photon Upconversion usually displays luminescent properties with decay times from hundreds nanoseconds to few milliseconds. A more recent investigation using upconversion nanoparticles as water sensor, single molecule image and Bioimaging and Bioassays shows the lifetime in the range of 150 µs to 800 µs [8][9][10]. The present data were acquired with Dr. Hsian-Ming Lee at the Institute of Chemistry, Academia Sinica (Taipei, Taiwan ROC) with the upconversion nanoparticle sample [11]. In this application notes, we presents the lifetime and Phosphorescence Lifetime Imaging (PLIM) measurement of such sample.

2 System Configuration and PLIM

The Phosphorescence Lifetime Imaging Microscopy (PLIM) is a very useful tool to localize the phosphorescence probes based on their lifetimes to study the variation in the lifetimes due to the micro environment changes [12]. We analyze the data with the phasor plot [13] [14], which is a graphic representation of the raw PLIM data in a vector space. The PLIM acquisition can be single point or a 2D image. With single point, we acquire a time series of raw data vs time and find out the decay times using the phase histogram [15] time-tagged time-resolved fitting approach. The result is used to calibrate the PLIM. The ISS data acquisition unit FastFLIM allows for changing the laser excitation repetition rates (usually from 80 MHz to 1 Hz), the duty cycle (usually 5%), and the mode (“burst”, good for laser diodes, or “non-burst”, good for CW laser On/Off control input).

Figure 1 shows the schematic of the PLIM setup, implemented on an ISS Alba confocal laser scanning microscopy system (www.iss.com/microscopy/instruments/alba.html). The Alba is coupled to a Nikon Ti-U microscope equipped with a Nikon 60X/1.2NA water objective lens. Galvo mirrors are used for the XY scanning of samples, and the optical

sectioning is performed by mounting the objective lens on a piezo-Z device (MadCity Labs). The scanning and piezo devices are synchronized to the FastFLIM data acquisition unit. The typical detectors used by Alba (up to 4 channels) are GaAsP (Model H7422P, by Hamamatsu) or Hybrid (Model R10467, by Hamamatsu) photomultiplier tubes (PMTs) or single photon counting module (SPCM, by Excelitas) avalanche photodiodes (APDs); the 2-channel Alba system used for these measurements is equipped with the SPCM-ARQH-15 APD detector in channels 1 and 2. Both data acquisition and analysis are performed using the ISS VistaVision 64-bit software.

A 980-nm CW laser (MDL-III-980L-150mW, Changchun New Industries Optoelectronics Technology Co., Ltd. www.cnilaser.com) is modulated with frequencies in the range 100 KHz - 250 Hz with a 5% duty cycle pulses by ISS FastFLIM unit for time-tagged time-resolved measurements. The 980-nm excitation laser is mounted on the ISS 3-laser laser launcher for its intensity control, and then delivered to the Alba system via a single mode polarization-maintained fiber (Oz-Optics).

In Alba, the excitation beams pass through the excitation dichroic (D2, 488/561/635/2p, Chroma) that reflects the de-scanned emission light. For PLIM measurements, an emission dichroic (D3, Glass, Chroma) is used to pass all the emission signal to channel 1. In channel 1, the emission light is filtered by a 720sp/2p emission filter (Chroma). A motorized, variable-aperture, confocal pinhole set at 70 µm diameter, is placed before the Ch1 detector.

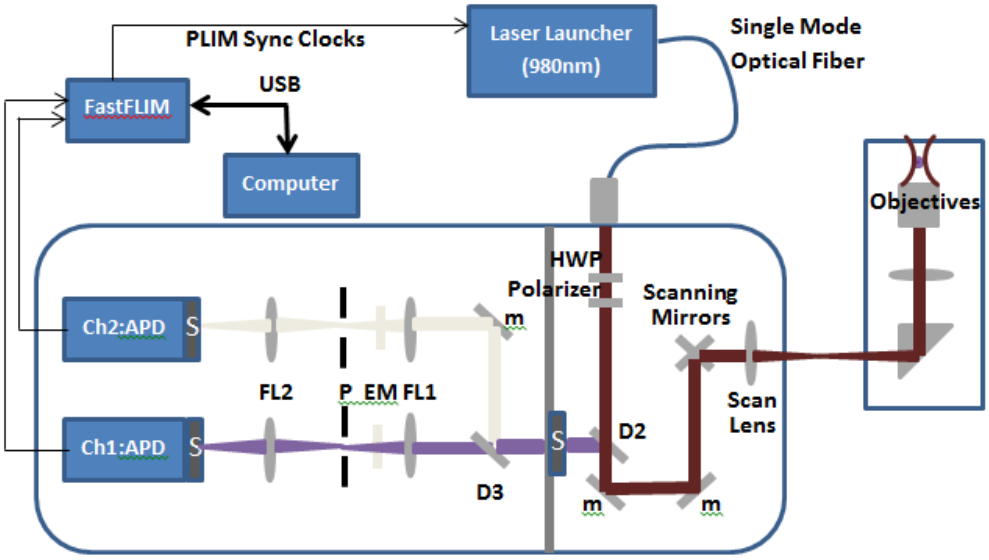

Figure 1: The PLIM system setup.

3 Upconversion Nano Particles Emission Spectrum, Excitation at 980nm

Figure 2 shows the emission spectra of the nanoparticles at two values of the excitation laser power. Specifically, if the excitation laser power is doubled the intensity of the emission lines increases by about 4 times.

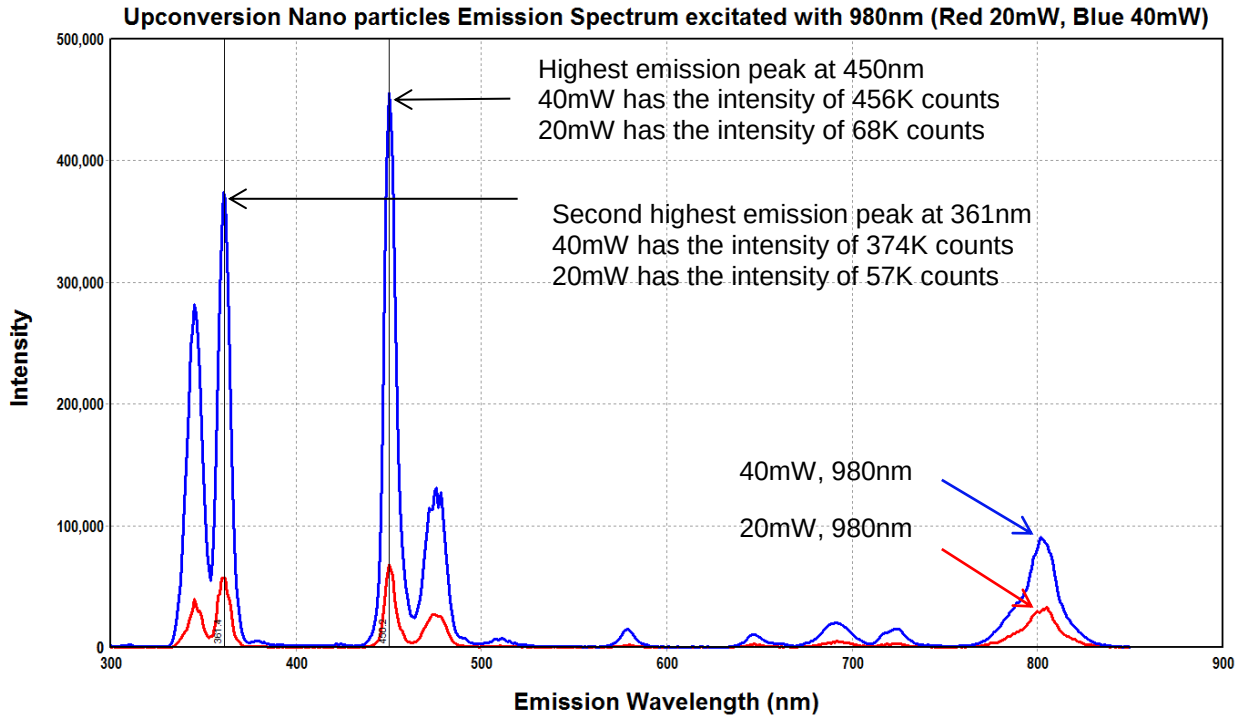

Figure 2: Upconversion nanoparticles emission spectra at 20mW and 40mW laser power. Excitation wavelength is 980 nm. Excitation power: 20mW (red), 40mW (blue). Emission peaks are 345nm, 361nm, 450nm, 475nm, 510nm, 578nm, 647nm, 693nm, 724nm, 802nm.

4 Upconversion Nano Particles Counts per Second vs Laser Power

Figure 3 shows the relationship between Counts per Second and Laser Power for the upconversion nanoparticles. As the 980nm laser has a maximum 160mW CW output, we modulate it at 250 Hz (5% duty cycle) or 1 KHz (5% duty cycle) for the PLIM measurements.

laser power		
%	µW	cps
0	0	0.02
10	0.8	0.05
20	1.5	0.12
30	3.8	1.6
40	12	1.8
50	37.8	125
60	136.5	830
65	305	
70	1049	
80	1878	
90	1850	
100	1755	

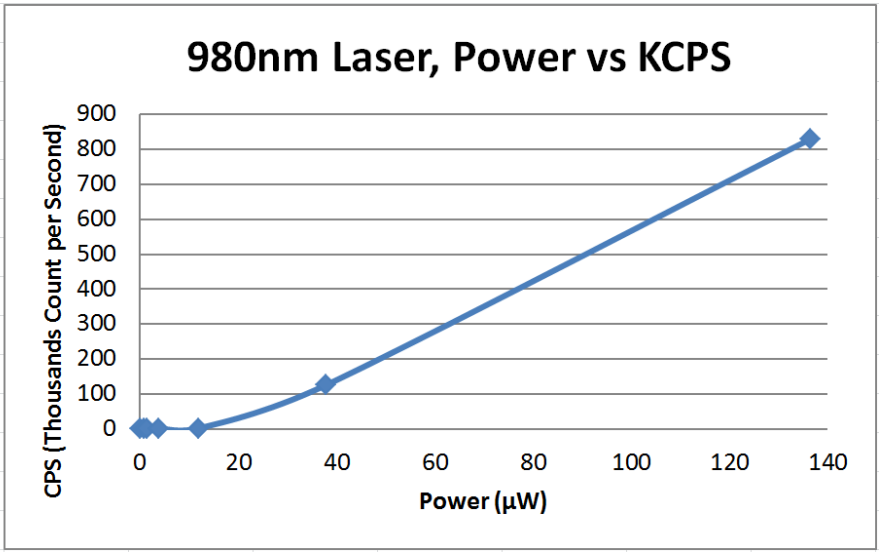

Figure 3: Upconversion Nanoparticles Counts per Second vs Laser Power. We use up to 60% of power, which is 140 µW (or about 7% of the maximum power), and the counts get to 830K CPS.

The power at the output of the optical fiber is 40%; that is, with the 5% duty cycle, the power is 160mW * 40% * 5% = 3.2mW, and with further optical loss, a 1.9mW was measured at the entrance of Alba microscopy system. Even with the 1.8mW, we have not used the full power to excite the upconversion nanoparticles; this shows the high efficiency energy transfer in the upconversion nanoparticles.

5 Measurements results from time tagged time resolved FFS mode and PLIM

Figure 4 shows the single point measurement of time-tagged time-resolved FFS measurement acquired for 30 seconds. The excitation frequency is 250 Hz, the resolution of the histogram data is actually 1,024,000, but we bin to 4096 points to present the phase histogram, which is actually the time domain decay data. We fit with time domain fitting routines and we get 280 µs for the phosphorescence lifetime.

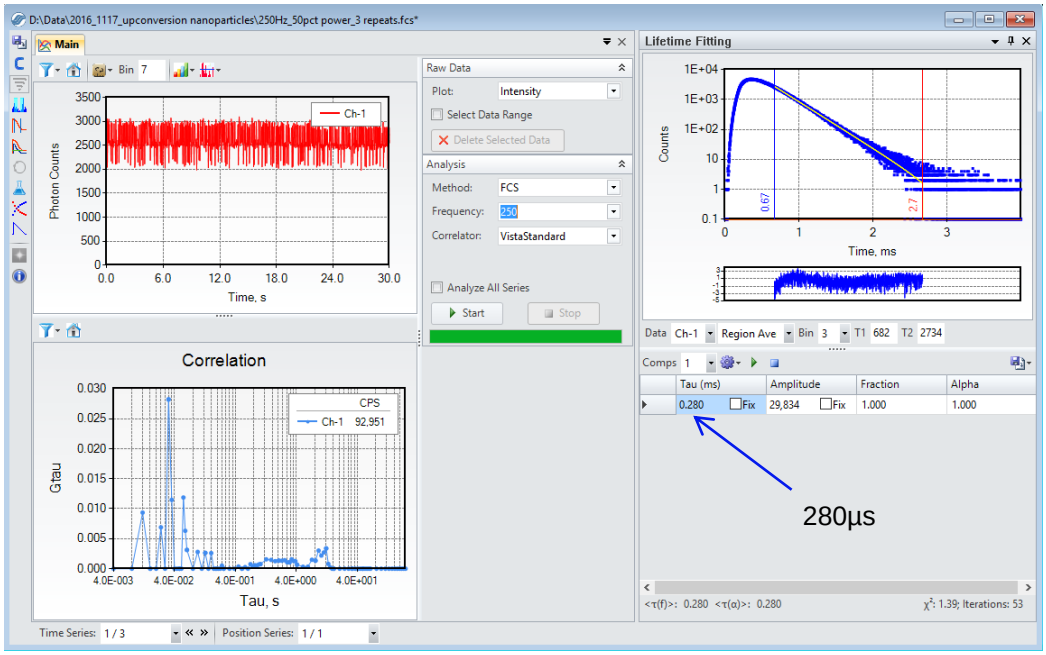

Figure 4: Using time tagged time resolved phase histogram for a direct time domain fit, found the 280µs lifetime.

Figure 5 shows the PLIM measurement with 256x256 pixel resolution, acquired with a dwell time of 8 ms per pixel (acquisition time is about 9 minutes). The excitation frequency is 250 Hz, and is calibrated with lifetime of 280 µs. We fit the phase modulation of phosphorescent lifetime of 272 µs.

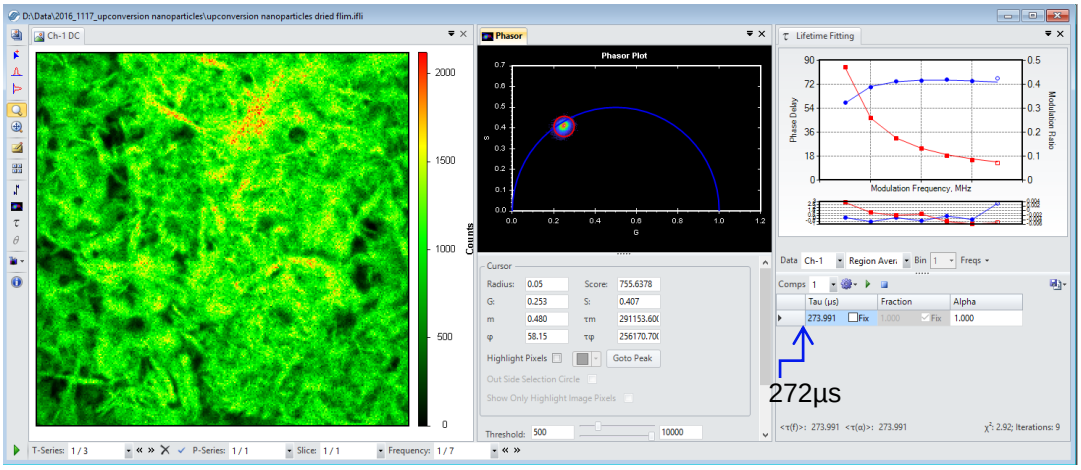

Figure 5: PLIM measurement of about 9 minutes, found the 272µs lifetime.

6 PLIM FRET

Upconversion nanoparticles sample of channelrhodopsin-ucnp is used to measure the PLIM FRET. The excitation wavelength of ucnp is 980nm and the emission is at 453nm and 474nm. The excitation wavelength of channelrhodopsin is 450nm-470nm, but channelrhodopsin won't show any emission.

6.1 channelrhodopsin-ucnp PLIM

Figure 6 shows the PLIM of channelrhodopsin-ucnp. There are shorter lifetime regions, which is an indication of a higher FRET efficiency: the lifetime has a major distribution around 230 µs and the shorter lifetimes are around 200 µs. The fitting of the donor-acceptor lifetime using two components fit. For example, a lifetime fit of 244 µs at cursor location is actually contain 149 µs (78%) and 585 µs (22%). The FRET efficiency is determined by using the FRET calculator of the VistaVision software (as described in next section).

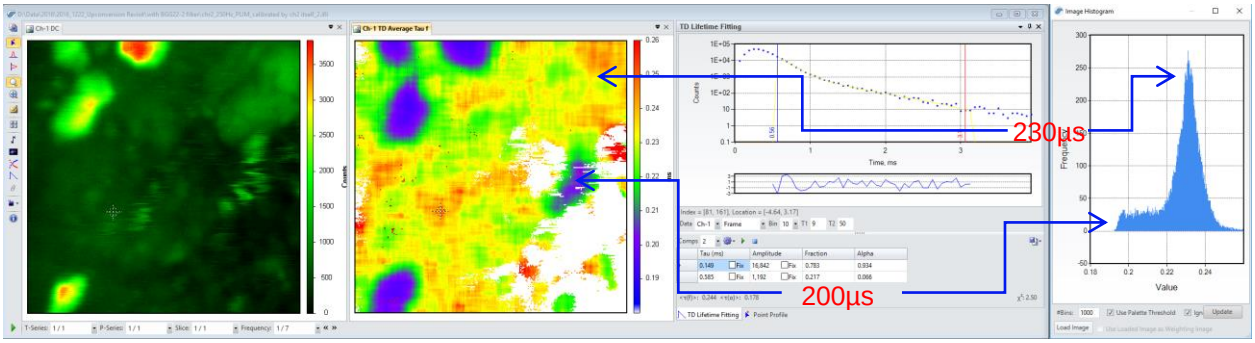

Figure 6: PLIM of channelrhodopsin-ucnp.

6.2 PLIM FRET Phasor Analysis

Figure 7 below shows the PLIM Phasor Analysis of channelrhodopsin-ucnp (positive control). The 220 µs decay time is assigned to the donor only while the FRET distribution is centered at 125 µs. Assuming the background has a longer decay time, we then find the FRET efficiency to be about 47% from the analysis using the FRET calculator.

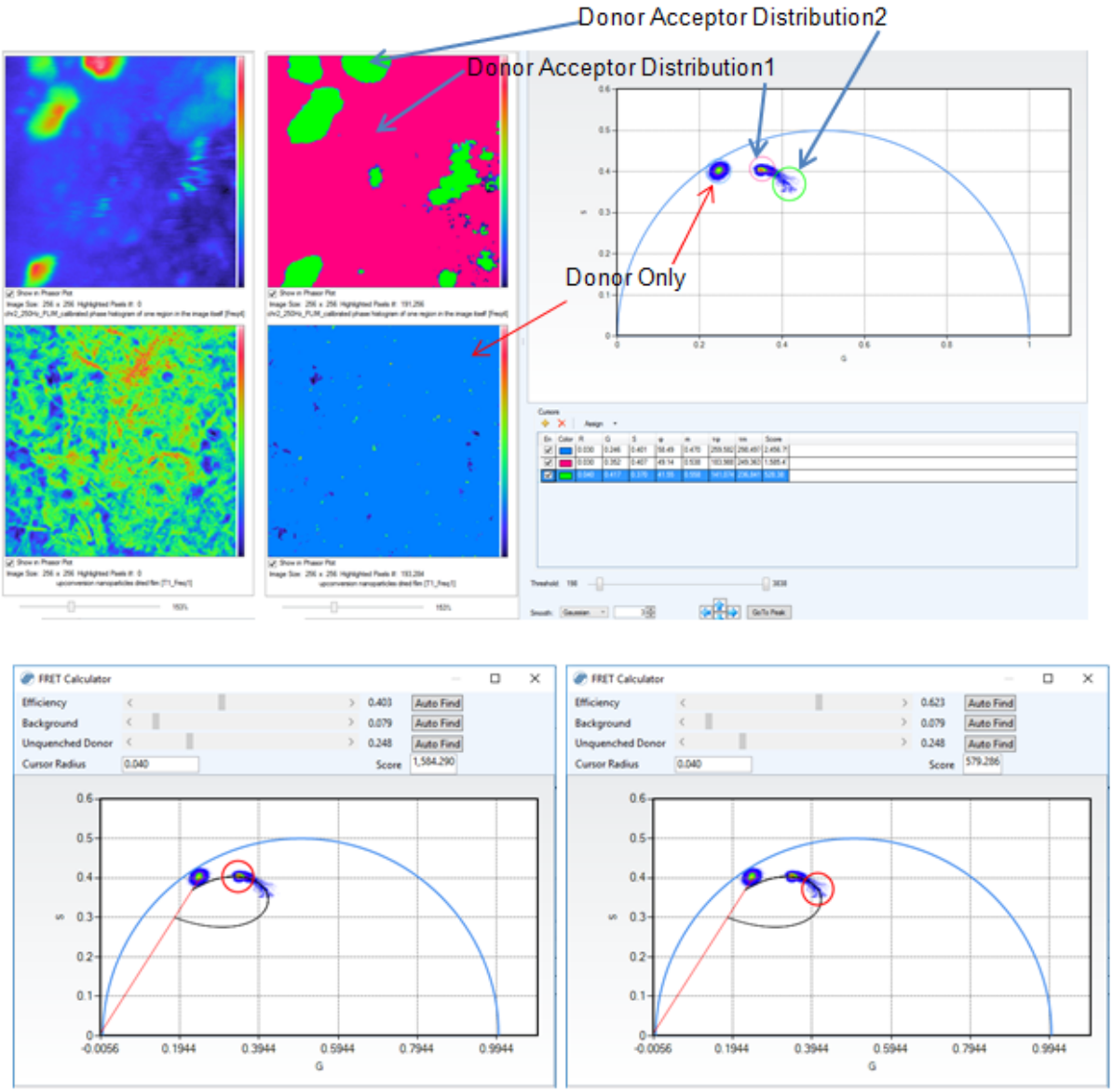

Figure 7: PLIM analysis of FRET efficiency of 40% to 62%

7 Conclusions

With the FastFLIM acquisition unit one can easily investigate different phosphorescent lifetimes ranging from few hundreds nanoseconds (set to 1 MHz excitation pulse rate) to a few milliseconds (set to 250 Hz excitation pulse rate, for example). The fitted lifetime are used as a reference for further PLIM measurements. The FRET analysis routine provides the FRET efficiency.

The benefits of FastFLIM are manifold:

- The unit is capable of measuring both fluorescent and phosphorescent lifetimes.
- Easy to work with continuous wave (CW) lasers that can be modulated over a wide range of frequencies (80MHz to 0.0596Hz). The frequency, duty cycle and burst or non-burst mode can be easily changed in the software.
- FFS time-tagged-time resolved mode can be analyzed with FCS, PCH, phasor plot, frequency domain fit and time domain (phase histogram) fit, as so called “multi-parameter” analysis [16].
- Phosphorescent FRET data can be easily analyzed with the FRET calculator.

Acknowledgements

We greatly thank Dr. Hsien-Ming Lee and Dr. Lee’s laboratory team, Tzu-ho Chen and Hua-De Gao (Institute of Chemistry, Academia Sinica, Taipei, Taiwan, R.O.C.) for providing the nanoparticles sample.
We also thank Changchun New Industries Optoelectronics Technology Co., Ltd. P.R. China, for providing the 980nm laser.

References

[1] Bo Zhou, Bingyang Shi, Dayong Jin & Xiaogang Liu. *Controlling Upconversion nanocrystals for Emerging Applications*. Nature Nanotechnology. 10:924-936 (2015).

[2] Haase, M.; H. Schäfer. *Upconverting Nanoparticles*. Angewandte Chemie International Edition. **50**: 5808–5829 (2011).

[3] Auzel, François. *Upconversion and Anti-Stokes Processes with f and d Ions in Solids*. Chem. Rev. **104** (1): 139–174 (2004).

[4] Gamelin, Daniel, R. Güdel, U. Hans. *Design of Luminescent Inorganic Materials: New Photophysical Processes Studied by Optical Spectroscopy*. Acc. Chem. Res. **33** (4): 235–242 (2000).

[5] Huang, Zhiyuan; Li, Xin; Mahboub, Melika; Hanson, Kerry M.; Nichols, Valerie M.; Le, Hoang; Tang, Ming L.; Bardeen, Christopher J. *Hybrid Molecule–Nanocrystal Photon Upconversion Across the Visible and Near-Infrared*. Nano Letters. **15** (8): 5552–5557 (2015-08-12).

[6] Wu, Mengfei, Daniel N. Congreve, Mark W. B. Wilson, Joel Jean, Nadav Geva, Matthew Welborn, Troy Van Voorhis, Vladimir Bulović, Moungi G. Bawendi, Marc A. Baldoi. *Solid-state infrared-to-visible upconversion sensitized by colloidal nanocrystals*". Nature Photonics, 10, (2016) 31-34.

[7] Kwon OS, Song HS, Conde J, Kim HI, Artzi N, Kim JH. *Dual-Color Emissive Upconversion Nanocapsules for Differential Cancer Bioimaging in vivo*. ACS Nano 26;10(1):1512-21. (2016 Jan 4).

[8] Liping Wei, Samer Doughan, Yi Han, Matthew V. DaCosta, Ulrich J. Krull and Derek Ho. *The Intersection of CMOS Microsystems and Upconversion Nanoparticles for Luminescence Bioimaging and Bioassays*. Sensors, 14, 16829-16855; doi:10.3390/s140916829 (2014).

[9] Daniel J. Gargas, Emory M. Chan, Alexis D. Ostrowski, Shaul Aloni, M. Virginia P. Altoe, Edward S. Barnard, Babak Sanii, Jeffrey J. Urban, Delia J. Milliron, Bruce E. Cohen1 & P. James Schuck. *Engineering bright sub-10-nm upconverting nanocrystals for single-molecule imaging*. Nature Nanotechnology, DOI:10.1038/NNANO.2014.29 (2014).

[10] Shaohong Guo, Xiaoji Xie, Ling Huang, and Wei Huang. *Sensitive Water Probing through Nonlinear Photon Upconversion of Lanthanide-Doped Nanoparticles*. ACS Applied Materials & Interfaces. 8, 847-853 (2016).

[11] Hua-De Gao, Pounraj Thanasekaran, Chao-Wei Chiang, Jia-Lin Hong, Yen-Chun Liu, Yu-Hsu Chang, and Hsien-Ming Lee. *Construction of a Near-Infrared-Activatable Enzyme Platform To Remotely Trigger Intracellular Signal Transduction Using an Upconversion Nanoparticle*. ACS Nano, 9 (7), pp 7041–7051. (2015).

[12] Ulas C. Coskun, Sandra Lam Yuansheng Sun, Shih-Chu Jeff Liao, Steve C. George, Beniamino Barbieri. *Frequency domain Phosphorescence Lifetime Imaging measurements and applications by ISS FastFLIM and multi pulse excitation*. Proc. SPIE 10069, Multiphoton Microscopy in the Biomedical Sciences XVII, 1006918 (February 21, 2017); doi:10.1117/12.2255481

[13] Yuansheng Sun and Shih-Chu Liao. *The Ultimate Phasor Plot and beyond*. ISS, Resources, Application Notes. (http://www.iss.com/resources/pdf/appnotes/Phasor_Plot_And_Beyond.pdf). (2016).

[14] Day, R. *Measuring Förster Resonance Energy Transfer Using Fluorescence Lifetime Imaging Microscopy*. Microscopy Today, 2015, 23(3), 44-51. (2015).

[15] Colyer, R.A., Lee, C. & Gratton, E. *A novel fluorescence lifetime imaging system that optimizes photon efficiency*. Microsc. Res. Tech. 71, 201–213 (2008).

[16] Yuansheng Sun, Ulas Coskun, Phoebe S. Tsoi, Josephine C. Ferreon, Allan Chris Ferreon, Beniamino Barbieri, Shih-Chu Jeff Liao, *Quantitative multi-parameter analysis of single molecule dynamics by PIE FastFLIM microscopy*. Proc. SPIE 10069, Multiphoton Microscopy in the Biomedical Sciences XVII, 100691X (February 21, 2017); doi.org/10.1117/12.2255961

.

For more information please call (217) 359-8681

or visit our website at **www.iss.com**

1602 Newton Drive
Champaign, Illinois 61822 USA
Telephone: (217) 359-8681
Fax: (217) 359-7879
Email: iss@iss.com